View metadata, citation and similar papers at core.ac.uk

brought to you by CORE

provided by Crossref

UNIVERSITY OF AMSTERDAM

UvA-DARE (Digital Academic Repository)

Using offset interfering beams for improved resolution in confocal imaging: the potential of the PSAF-technique

Müller, M.; Brakenhoff, G.J.

Published in:
Bioimaging

Link to publication

Citation for published version (APA):
Müller, M., & Brakenhoff, G. J. (1996). Using offset interfering beams for improved resolution in confocal imaging: the potential of the PSAF-technique. Bioimaging, 4(3), 179-186.

General rights
It is not permitted to download or to forward/distribute the text or part of it without the consent of the author(s) and/or copyright holder(s), other than for strictly personal, individual use, unless the work is under an open content license (like Creative Commons).

Disclaimer/Complaints regulations
If you believe that digital publication of certain material infringes any of your rights or (privacy) interests, please let the Library know, stating your reasons. In case of a legitimate complaint, the Library will make the material inaccessible and/or remove it from the website. Please Ask the Library: http://uba.uva.nl/en/contact, or a letter to: Library of the University of Amsterdam, Secretariat, Singel 425, 1012 WP Amsterdam, The Netherlands. You will be contacted as soon as possible.

UvA-DARE is a service provided by the library of the University of Amsterdam (http://dare.uva.nl)

Download date: 11 May 2019

Bioimaging **4** (1996) 179–186. Printed in the UK

Using offset interfering beams for improved resolution in confocal imaging: the potential of the PSAF-technique

M Müller and G J Brakenhoff

BioCentrum Amsterdam, University of Amsterdam, Department of Molecular Cytology. Kruislaan 316, 1098 SM Amsterdam, The Netherlands

Submitted 17 June 1996, accepted 4 November 1996

Abstract. The interferometric spatial overlap of two laterally offset focal field distributions of a high numerical aperture lens in combination with confocal detection lead to improved resolution in confocal imaging. Experimental data of the achieved signal, the point spread autocorrelation function (PSAF), are presented for both the lateral and axial directions. Numerical simulations of lateral PSAF imaging of selected fluorescent objects show an increased resolution of up to 30% with moderate ringing, obtainable also in the presence of moderate spherical aberrations.

Keywords: point spread function, lateral resolution, confocal imaging

1. Introduction

Over the last couple of years several approaches have been developed to increase the lateral and axial resolution of the light microscope. The confocal microscope [1–3] provides optical sectioning power thus permitting the separate recording of optical slices of an object and the subsequent reconstruction of a full three-dimensional image. It also provides an increased lateral resolution. Further improvement of the axial (and lateral) resolution is obtained through an increase of the effective numerical aperture (NA) of the microscope by using two microscope objectives from opposite sides. This so-called 4Pi-microscopy [4, 5] has the additional advantage that an almost spherical point spread function (PSF) is generated, which is helpful in restoration schemes [6] for further processing of the image data. A semi-spherical PSF is also obtained in 'theta' microscopy [7], where the illumination and detection pathway cross at a certain angle. In this manner an increased axial resolution is obtained, albeit for low NAs due to mechanical constraints of commercially available microscope objectives.

All these techniques may be combined with two-photon excitation [4, 8–11] to profit from an increased depth of penetration and reduced out-of-focus bleaching. Recently, several advanced schemes to modify the effective illumination PSF (e.g. [12, 13]) have been proposed for an extra improvement of the resolution. Basically, all these techniques rely on some sort of non-linear excitation and/or detection scheme that changes the effective shape of the PSF to provide an increase in resolution.

In this paper we present some recent experimental and theoretical results on the point spread autocorrelation function (PSAF) technique [14–16], which can be used for obtaining an increase in resolution over confocal, for both the lateral and axial directions. The technique—which relies on the detection of the fluorescence generated by the cross-product of two illuminating amplitude PSFs—is inherently robust because it uses a common path interference arrangement. Also, no special specimen preparation is required, nor are there any restrictions on the fluorescing dyes which can be used. These aspects allow for a relatively straightforward incorporation of the technique in a standard confocal microscope.

Shortly after the first publication of the PSAF technique [14], Vaez-Iravani *et al* published a conceptually similar method for resolution improvement in scanning microscopy [17]. Their approach is based on the generation of a beat frequency in the overlap region of two spatially shifted focal spots. The two methods, which have been developed almost simultaneously in two different laboratories, will be compared in section 4.

0966-9051/96/030179+08$19.50 © 1996 IOP Publishing Ltd

This paper is organized as follows. In section 2 the principle of the PSAF technique is explained and experimental results are presented of the measurement of the lateral and axial PSAF signals. In section 3 the possible improvement of the lateral resolution is analysed theoretically for some example specimens. Also, the influence of aberrations on the PSAF response is investigated. Section 4 concludes this paper with a discussion of the results.

2. The PSAF technique

2.1. Principle of the technique

The PSAF technique is based on an interferometric superposition of two laterally offset illumination distributions (PSFs) at the focal point of a high NA objective. The two illumination distributions can be shifted both laterally and axially with respect to each other. Furthermore, the response is detected confocally, where the conjugate detection distribution can be positioned at a certain point in the specimen relative to the illumination distributions.

Imagine the complex focal field of a high NA objective to consist of two (complex) parts—a 'reference' field u_{ref} and an 'object' field u_{obj}—of which the relative spatial position and phase can be controlled. If part of the radiation is absorbed by an object, described by the object function $O(\boldsymbol{r})$, re-emitted as fluorescence and detected through a detection distribution characterized by $|u_{det}|^2$, then the time-averaged and space integrated fluorescence signal is given by:

$$G(\Delta\boldsymbol{r}_1, \Delta\boldsymbol{r}_2, \Delta\phi) = \int_{-\infty}^{\infty} \mathrm{d}\boldsymbol{r}\ O(\boldsymbol{r}) \cdot |u_{ref}(\boldsymbol{r}, \phi_0) + u_{obj}(\boldsymbol{r} + \Delta\boldsymbol{r}_1, \phi_0 + \Delta\phi)|^2 \cdot |u_{det}(\boldsymbol{r} + \Delta\boldsymbol{r}_2)|^2. \quad (1)$$

In equation (1), $\Delta\boldsymbol{r}_1$ and $\Delta\boldsymbol{r}_2$ denote the focal shifts of the object illumination and the conjugate detection distribution respectively, relative to the reference illumination distribution, ϕ_0 denotes an arbitrary phase offset and $\Delta\phi$ denotes a relative phase difference between the object and reference field. The PSAF technique is based on detecting the difference signal between two relative phase conditions between the reference and object focal field:

$$I_{\mathrm{PSAF}}(\Delta\boldsymbol{r}_1, \Delta\boldsymbol{r}_2, \Delta\Phi) = G(\Delta\boldsymbol{r}_1, \Delta\boldsymbol{r}_2, \Delta\phi_1) - G(\Delta\boldsymbol{r}_1, \Delta\boldsymbol{r}_2, \Delta\phi_2) \quad (2)$$

where $\Delta\Phi = \Delta\phi_1 - \Delta\phi_2$. It is the cross-product term in equation (1) that provides the basis for an increase in imaging resolution.

A practical arrangement for obtaining the PSAF signal, as described above, is shown schematically in figure 1.

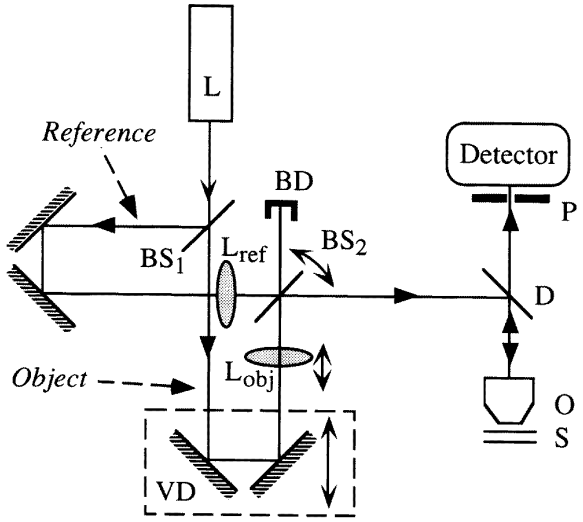

Figure 1. Schematic of the experimental set-up, with L: laser; BS: 50% beamsplitter; VD: variable delay; Lref, Lobj: lens in reference and object beam respectively; BD: beam dump; D: dichroic mirror; O: microscope objective; S: sample; P: confocal pinhole.

A laser beam is split into two parts—the reference and object beams—by a 50% beamsplitter (BS1). The object beam passes a variable delay line (VD), before being recombined with the reference beam on a second 50% beamsplitter (BS1). Changing the variable delay introduces a difference in optical path length between the two beams and hence influences the relative phase. The two beams (parallel and collinear) are reflected off a dichroic mirror (D) and focused into a fluorescing sample (S) by a high NA objective (O). The fluorescence is monitored in the back-scattering direction, through the dichroic mirror and a confocal pinhole (P), with a photodetector. A tilt of the second beamsplitter induces a lateral shift of the object PSF with respect to the reference PSF. Additionally, a translation of the lenses Lref and Lobj provides a relative axial shift of the illumination distributions with respect to each other and with respect to the conjugate confocal detection distribution. Note that in a first approximation the two illumination distributions are equal (apart from a spatial shift), whereas the detection distribution will in general be different due to the Stokes shift between the excitation and emission wavelength of the fluorescing dye.

In a straightforward implementation of the PSAF technique—given by equations (1) and (2)—the variable delay can either be driven sinusoidally, inducing a periodic phase change of the object beam with respect to the reference beam, or alternate between two specific phase conditions, e.g. inducing a phase difference between the two beams of either 0 or π. In these cases, either the amplitude of the fluorescence oscillations or the difference in the fluorescence signals between the two phase conditions can be measured.

2.2. Lateral and axial PSAF

It follows from a straightforward qualitative argument that the PSAF signal depends on the shape of the underlying intensity PSF. As is well known, there is a π phase jump at every node in the lateral direction of the complex PSF in the focal plane. When the PSFs of the reference and object beam coincide, the two fields will have an identical spatial phase relation and the fluorescence generated by the interfering fields will be strongly modulated when the relative phase of the object beam is varied. However, when the object PSF is shifted laterally with respect to the reference PSF, some zones along the lateral coordinate will have equal phase, while others will have opposite phase. Hence, with a varying relative phase of the object beam with respect to the reference, different zones will interfere in a different manner. It can be shown [15], that for certain focal shifts the integrated fluorescence signal is independent of the relative phase delay between the reference and object beam, yielding a PSAF signal equal to zero.

As an experimental demonstration of this effect, the lateral and axial PSAF signals are shown in figure 2. Both have been determined within the bulk of a fluorescing solution (approximately 5 μm below the interface). The specific experimental conditions of the two measurements are slightly different and are described in detail elsewhere [15, 16]. Clearly the PSAF signal is similar in shape to the underlying PSF, including the sidelobe structure. The positions of the nodes are found to be close, but not equal, to the node positions in the generating PSF. The PSAF signal shows a strong dependence on the intensity profile of the illuminating beams across the aperture of the objective. For example, the full width half maximum (FWHM) of the experimental PSAF signal is plotted in figure 3, as a function of the effective NA of the objective. Note that for high NA the lateral FWHM is smaller than the axial FWHM by a factor of approximately three. Also, the axial FWHM increases rapidly (square dependence) with decreasing NA, whereas the lateral FWHM increases almost linearly with decreasing NA.

These results show the potential of the PSAF technique for the determination and optimization of the illumination conditions of high NA objectives or more complex optical systems. The technique only requires a simple sample consisting of a solution of a fluorescing dye. Since the interferometric arrangement is basically common path, the technique is inherently robust.

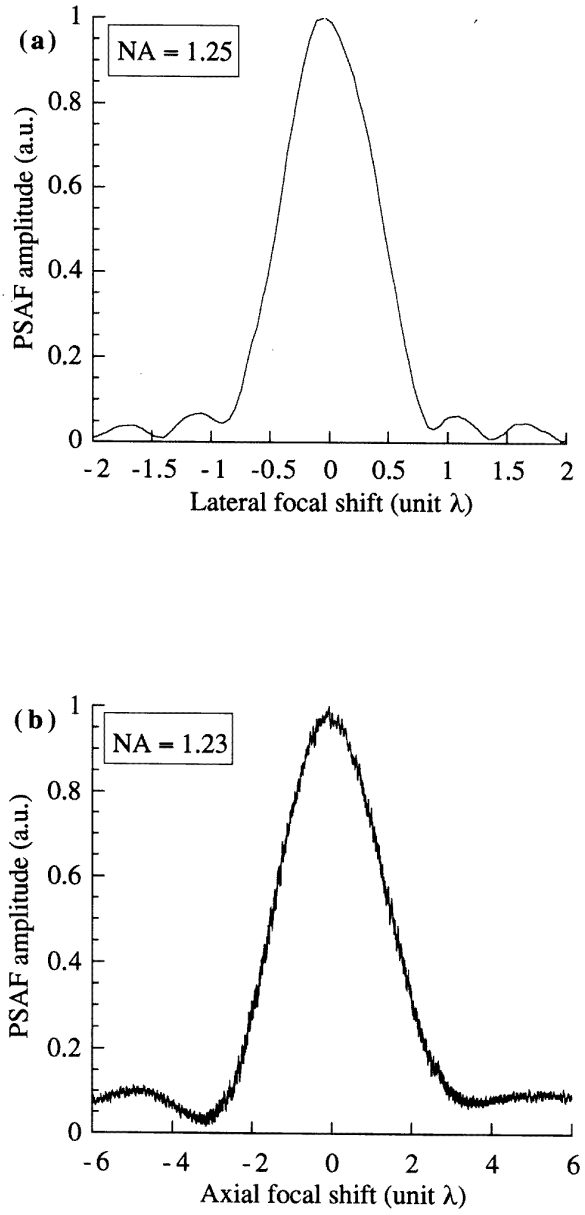

Figure 2. Measurement of the PSAF signal. In both cases the sample consisted of a 10-3 M solution of Rhodamine 6G in water contained in a microslide (Vitro Dynamics, NJ). (a) Lateral PSAF signal. A three-element compound objective (Leitz: Oil, Plan 100, NA= 1.25) was used, without confocal detection. (b) Axial PSAF signal. A Leitz 63/1.3–0.6 oil objective was used, with a 10 μm confocal pinhole to realize a conjugate detection distribution positioned midway between the reference and object illumination PSFs.

3. Improvement of resolution in PSAF imaging

With a slight modification of the technique, the PSAF signal can also be used for the imaging of structured fluorescent distributions that are present in labelled biological objects, for instance. It has been demonstrated [16] that an improved axial resolution over confocal microscopy can be realized by PSAF imaging with a resolution improvement of approximately 30% . In this section we will theoretically investigate the resolution improvement by PSAF imaging in the lateral direction. Furthermore, we will show that the same principle of resolution improvement holds for the case of imaging with PSFs which suffer from moderate spherical aberration.

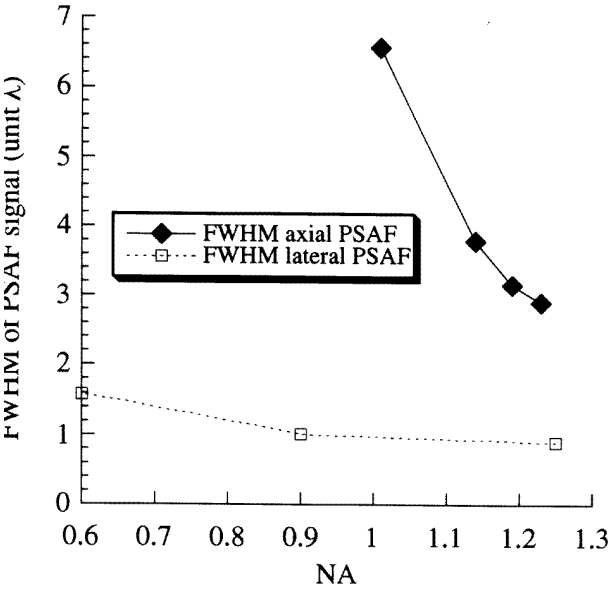

Figure 3. FWHM of the experimental lateral and axial PSAF signals as a function of the effective NA of the objective. The experimental conditions are the same as described in figure 2.

3.1. Theoretical model

The modelling of the PSAF signal response to a fluorescing object is based on a calculation of the (complex) PSF of a high NA lens. In our calculations we have used a numerical evaluation of the first Rayleigh–Sommerfeld integral of scalar diffraction theory [18, 19]. The shift invariance approximation is used to incorporate the lateral focal shift of the object beam with respect to the reference beam. The relatively small focal shifts and the high quality flat field of modern microscope objectives justify this approximation. For simplicity, we have considered the confocal detection PSF equal to that of the illumination ($u_{ref} = u_{obj} = u_{det}$, see equation (1)), thereby neglecting the shift in wavelength between excitation and emission. However, this only yields a response which is slightly steeper than the actual response, but does not influence the basic principle of resolution increase through PSAF imaging. In the following calculations the conjugate confocal detection distribution is positioned midway between the reference and object illumination distribution ($\Delta \boldsymbol{r}_2 = \frac{1}{2}\Delta \boldsymbol{r}_1$, see equation (1)).

It follows from equation (2) that the PSAF signal can be determined in a number of ways, depending on the actual phase difference interval taken. For the calculations presented here, the PSAF signal is defined as the difference between maximum intensity and the minimum intensity generated for phase delays of the object beam relative to the reference beam between 0 and 2π:

$$I_{PSAF}(\Delta \boldsymbol{r}) = \mathrm{Max}(G(\Delta \boldsymbol{r}, \Delta\phi);\ \Delta\phi \in [0, 2\pi]) - \mathrm{Min}(G(\Delta \boldsymbol{r}, \Delta\phi);\ \Delta\phi \in [0, 2\pi]). \quad (3)$$

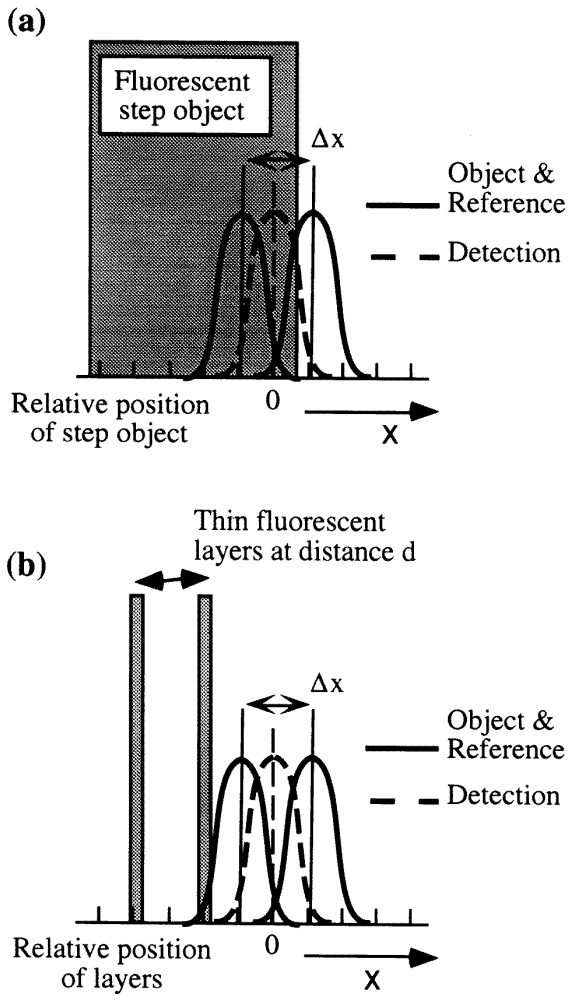

Figure 4. Schematic layout for modelling the PSAF response to two fluorescing objects. (a) One-sided fluorescing step. (b) Two thin fluorescent layers. The object illumination PSF is shifted with a focal shift Δx with respect to the reference. The conjugate confocal detection distribution is positioned midway between the two illuminating distributions.

Two example objects have been used in the calculations: a single sided fluorescing step object and two thin fluorescing layers. Figure 4 shows a schematic of the model systems. The PSAF response for a certain focal shift is calculated from an evaluation of equation (3) as a function of the object position. This process is then repeated for a number of focal shifts.

3.2. PSAF imaging of example fluorescing objects

When considering imaging with the PSAF signal it is essential to realize that there is in fact not a unique 'PSAF' image, but rather a 'family' of PSAF images, with each image collected at a certain focal shift, $\Delta \boldsymbol{r} = (\Delta x, \Delta y, \Delta z)$, between the two generating field

distributions. The possible degree of improvement in resolution using PSAF imaging depends sensitively on the PSAF focal shift used, and also requires confocal detection. In these model calculations we confine ourselves to the lateral case $\Delta \boldsymbol{r} = \Delta x$ (with lateral referring to the x- or y-axis and axial referring to the z-axis). The PSAF response is determined as a function of the object position along the x-axis. In figure 5(a) the family of PSAF responses to a single sided fluorescing step, defined by:

$$O(x) = \begin{cases} 1 & \text{if } x \geqslant 0 \\ 0 & \text{if } x < 0 \end{cases} \tag{4}$$

is shown for a number of lateral focal shifts. The optical axis is located at $(x = 0, y = 0)$ and the confocal detection distribution is centred at $(x = 0, y = 0, z = 0)$. The PSAF response for the shift value $\Delta x = 0$ is identical to the normal confocal response with a field distribution described by the underlying intensity PSF and can thus serve as a reference for comparing PSAF imaging with regular confocal imaging. As a rule of thumb, the distance between the 25% and 75% amplitude level of the response is comparable to the FWHM of the underlying PSF [20]. This distance—or steepness—is plotted in figure 5(b) as a function of the lateral focal shift. Note that for $\Delta x = 0$ the PSAF response is equivalent to the conventional confocal fluorescence response. Clearly the steepness of the response increases with increasing focal shift, accompanied by moderate ringing of the response (figure 5(a)).

An effective way to illustrate the improved resolution capabilities of the PSAF imaging technique is to calculate the minimum distance at which two thin fluorescent layers can be resolved. According to the Rayleigh criterion an intensity drop of 20% between the imaged layers is required. In figure 6 this relative drop in intensity is plotted as a function of the distance between the two layers for several focal shifts between the reference and object beam. In this case the fluorescent object function is given by:

$$O(x) = \begin{cases} 1 & \text{if } x = \pm\frac{d \pm \delta x}{2} \\ 0 & \text{otherwise} \end{cases} \tag{5}$$

where d is the distance between the two layers, each with a thickness δx which is much smaller than the lateral width of the PSF. Again, the case of $\Delta x = 0$ is equivalent to conventional confocal imaging. Judging from the PSAF response at a focal shift of $\Delta x = 0.7\lambda$, an increase in resolution of approximately 30% can be realized, with moderate ringing. The presence of ringing will not interfere with the possibility of discrimination in a simple two layer system. It may however introduce an element of uncertainty, increasingly so for more pronounced ringing, in the interpretation of fine structure in structurally more complex objects.

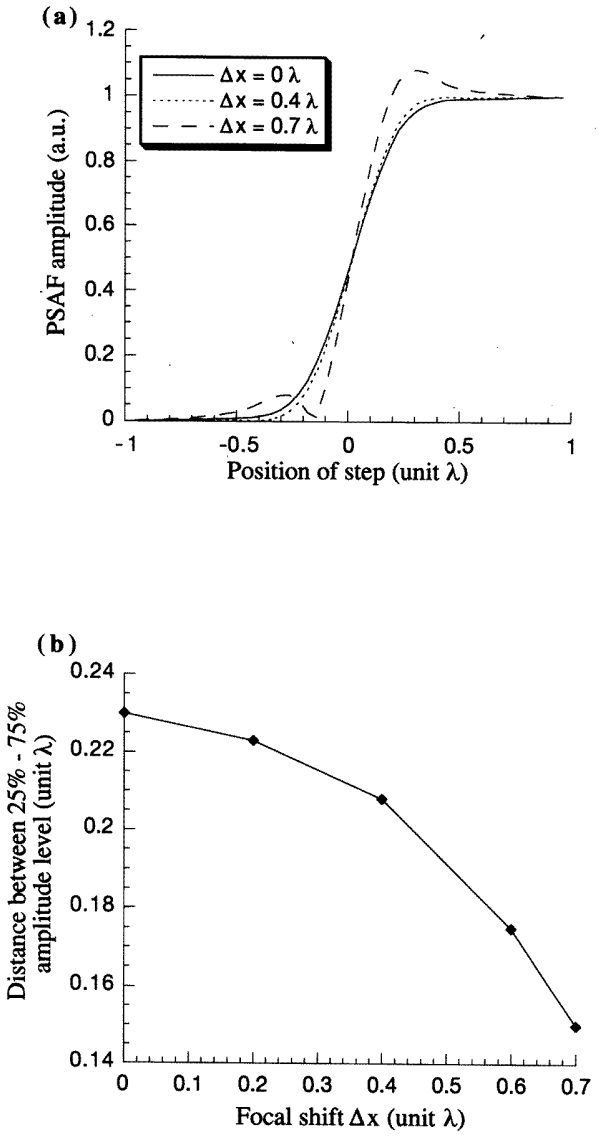

Figure 5. (a) Family of theoretical PSAF responses to a fluorescent lateral step for different values of the lateral focal shift Δx (in unit wavelength) between the reference and object beam. The signals are calculated for an objective with a semi-aperture angle of 60°. (b) The steepness—expressed as the distance between the 25% and 75% amplitude level—of the lateral PSAF response to a fluorescing step object as a function of the focal shift between the reference and object PSF.

3.3. PSAF imaging in the presence of spherical aberration

Several types of aberration may affect the PSF of a high NA lens. Of these, spherical aberration is possibly the most common in practical microscopy, resulting from either improper illumination of the objective or from a mismatch in the refractive index of the specimen [21–25]. To analyse the effect of this type of aberration on the PSAF imaging

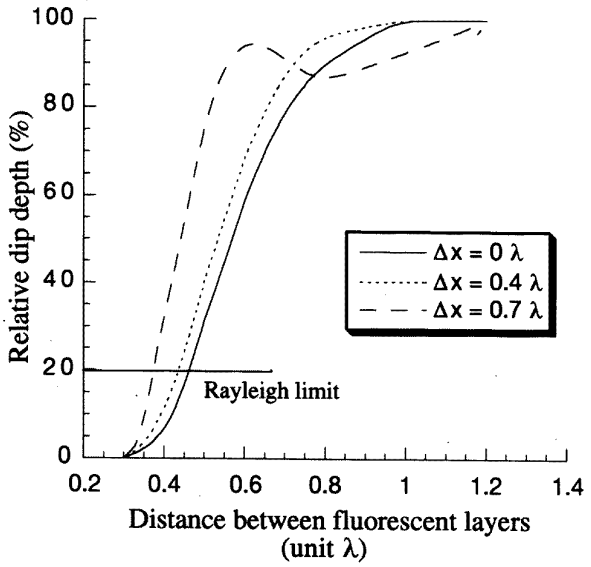

Figure 6. Relative depth of the dip in the PSAF response to two thin fluorescent layers as a function of the distance d, in unit wavelength, between them, for different values of the focal shift Δx between the reference and object beam. The relative dip size is expressed as the difference between the response value at the maximum and at the dip, divided by the response value at the maximum in the PSAF response. The signals are calculated for an objective with a semi-aperture angle of 60°.

principle, we calculated PSAF step responses based on a moderately aberrated PSF, where a spherical aberration of three wavelengths for the marginal ray was assumed in the scalar diffraction calculation. The results of these calculations are plotted in figure 7. Due to the aberrated PSF the steepness of the lateral PSAF response to a single sided fluorescing edge decreased by approximately 20%. Introducing a focal shift between the reference and the object beam again results in an increase of the steepness of the response. A comparison of figures 5(b) and 7(b) demonstrates that the presence of spherical aberration does not influence the relative improvement in resolution, even if the overall steepness of the response is reduced by the aberrations.

4. Discussion

In our numerical simulation of lateral PSAF imaging we have found that for certain types of objects, improved imaging can be expected with an increase in resolution of up to 30% with limited artefacts due to ringing. A comparable increase in resolution for axial PSAF imaging is predicted by our numerical simulations (data not shown). This theoretical prediction is confirmed by our recent experimental results which showed an increased steepness of the PSAF response to an axial one-sided fluorescent

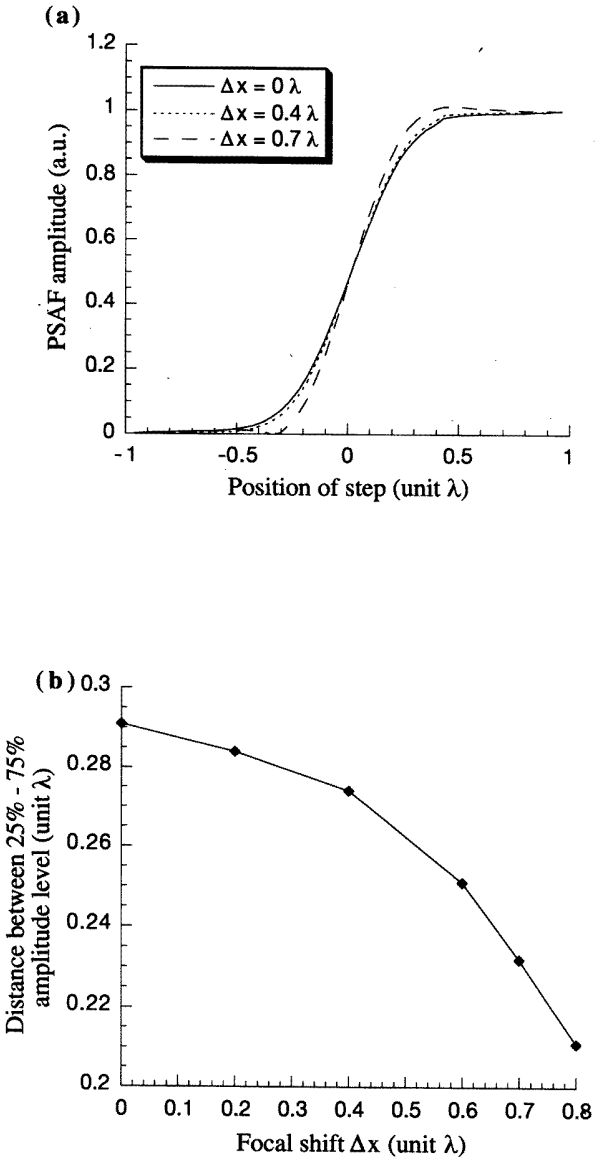

Figure 7. PSAF response calculated for generating PSFs which have moderate spherical aberration of three unit wavelengths for the marginal ray. (a) Family of theoretical PSAF responses to a fluorescent lateral step for different values of the lateral focal shift Δx (in unit wavelength) between the reference and object beam. The signals are calculated for an objective with a semi-aperture angle of 60. (b) The steepness—expressed as the distance between the 25% and 75% amplitude level—of the lateral PSAF response to a fluorescing step object as a function of the focal shift between the reference and object PSF.

step object [16]. The improved imaging capabilities of the PSAF technique—as numerically simulated for the lateral case—also apply to the case of imaging with PSFs that show moderate spherical aberrations. Further improvement of the theoretical model, such as including the vectorial properties of the field, is required to enable a full quantitative comparison of the theorical predictions

and the experimental results.

The presented results can be seen as a first step towards a wider investigation on the potential of the use of laterally and axially shifted PSAF signals for obtaining structural information at higher spatial frequencies than available in regular confocal microscopy. As each point in space can be interrogated at a number of PSAF conditions, each chosen with a spatial shift to optimize the response to a particular spatial frequency, it may well be that in this manner imaging can be realized with a zero-free extended spatial frequency transfer function. Whether this indeed turns out to be possible awaits further analysis, but given the presented results we think that this expectation will at least be realistic for spatial objects of limited extent, i.e. with dimensions on the order of a few times the half width of the focal distribution. Such selected sampling of the spatial frequencies at specific PSAF shifts offers good possibilities for further improved resolution in combination with proper deconvolution techniques even in the presence of 'zeros' in the effective transfer function [6, 26].

The PSAF technique is conceptually similar to the 'frequency-domain field confinement' technique, as developed almost simultaneously by Vaez-Iravani *et al* [17]. In this method the object and the reference beam, which have orthogonal polarization, are slightly shifted in frequency with respect to each other by two acousto-optic modulators. The focal spots of the two beams are then shifted laterally with respect to each other. In this configuration a rotating polarization is induced in the overlap area, at a rate equal to the beat frequency between the two beams. Since the excitation probability of a fluorophore depends on the orientation of its transition dipole moment relative to the polarization of the electric field, a fluorescence signal from a sample of equally oriented fluorophores will show a modulation at the beat frequency when generated in the overlap region of the two focal spots. In the non-overlapping regions only a DC fluorescence signal is generated.

Both the PSAF technique and the Vaez-Iravani technique use a modulation to enable detection of a signal from the overlap region of the focal spots only. Whereas PSAF uses an intensity modulation, generated by letting the two beams interfere and modulating the relative phase between them, the Vaez-Iravani technique employs a modulation of the polarization state of the field. Due to difference in the method of modulation, each of the two techniques has its own strengths and weaknesses. The PSAF technique is capable of analysing samples which have isotropically oriented fluorophores, a situation often encountered in biological specimen. In the case of strongly anisotropic samples, the PSAF signal strength becomes sensitive, not only to the fluorophore concentration, but also to the orientation of the dipole moments relative to the polarization of the fields. This ambiguity can be resolved by an additional measurement with both the reference and object field circularly polarized. The Vaez-Iravani technique, on the other hand, provides a sensitive measurement of the anisotropy of the sample. Highly isotropic samples will, however, average out the AC modulation and hence reduce the signal. Also, the required definition of polarization may reduce the attainable modulation depth in high-NA systems.

In summary, we have presented PSAF imaging, an approach towards improved resolution based on the interaction of two illuminating distributions combined with confocal detection. In contrast to 4Pi-imaging, the beams are delivered to the specimen in a common path arrangement, therefore offering a possibly more realistic and robust configuration with respect to propagation conditions for achieving improved image quality in optical microscopy.

Acknowledgement

This research was financially supported in part by the Stichting voor Fundamenteel Onderzoek der Materie, Utrecht, The Netherlands, under grant no. 94RG02.

References

[1] Sheppard C J R and Choudhury A 1977 Image formation in the scanning microscope *Opt. Acta* **24** 1051–73

[2] Brakenhoff G J, Blom P and Barends P 1979 Confocal scanning light microscopy with high aperture immersion lenses *J. Microsc.* **117** 219–32

[3] Brakenhoff G J, van der Voort H T M, van Spronsen E A, Linnemans W A and Nanninga N 1985 Three-dimensional chromatin distribution in neuroblastoma nuclei shown by confocal scanning laser microscopy *Nature* **317** 748–9

[4] Hell S and Stelzer E H K 1992 Fundamental improvement of resolution with a 4Pi-confocal fluorescence microscope using two-photon excitation *Opt. Commun.* **93** 277–82

[5] Hell S W, Lindek S, Cremer C and Stelzer E H K 1994 Measurement of the 4Pi-confocal point spread function proves 75 nm axial resolution *Appl. Phys. Lett.* **64** 1335–7

[6] van der Voort H T M and Strasters K C 1995 Restoration of confocal images for quantitative image analysis *J. Microsc.* **178** 165–81

[7] Stelzer E H K and Lindek S 1994 Fundamental reduction of the observation volume in far-field light microscopy by detection orthogonal to the illumination axis: confocal theta microscopy *J. Microsc.* **111** 536–47

[8] Denk W, Strickler J H and Webb W W 1990 Two-photon laser scanning fluorescence microscopy *Science* **248** 73–6

[9] Lakowicz J R, Gryczynski I, Gryczynski Z and Danielsen E 1992 Time-resolved fluorescence intensity and anisotropy decays of 2,5-diphenyloxazole by two-photon excitation and frequency domain fluorometry *J. Phys. Chem.* **96** 3000–6

[10] Piston D W, Sandison D R and Webb W W 1992 Time-resolved fluorescence imaging and background rejection by two-photon excitation in laser scanning microscopy *SPIE—Int. Soc. Opt. Eng.* **1640** 379–89

[11] Piston D W, Kirby M S, Cheng H, Lederer W J and Webb W W 1994 Two-photon-excitation fluorescence imaging of three-dimensional calcium-ion activity *Appl. Opt.* **33** 662–9
[12] Hell S W 1994 Improvement of lateral resolution in far-field fluorescence light microscopy by using two-photon excitation with offset beams *Opt. Commun.* **106** 19–24
[13] Hell S W and Wichmann J 1994 Breaking the diffraction resolution limit by stimulated emission: stimulated-emission-depletion fluorescence microscopy *Opt. Lett.* **19** 780–2
[14] Müller M and Brakenhoff G J 1995 Characterization of high-numerical-aperture lenses by spatial autocorrelation of the focal field *Opt. Lett.* **20** 2159–61
[15] Müller M and Brakenhoff G J 1996 Apodization and the point spread autocorrelation function *Appl. Opt.* in press
[16] Brakenhoff G J and Müller M 1996 Improved axial resolution by PSAF imaging *Opt. Lett.* **21** 1721–3
[17] Vaez-Iravani M and Kavaldjiev D I 1995 Resolution beyond the diffraction limit using frequency-domain field confinement in scanning microscopy *Ultramicroscopy* **61** 105–10
[18] Stamnes J J, Spjelkavik B and Pedersen H M 1983 Evaluation of diffraction integrals using local phase and amplitude approximations *Opt. Acta* **30** 207–22
[19] Stamnes J J 1986 *Waves in Focal Regions* (Bristol: IOP)
[20] Stelzer E H K, Hell S, Lindek S, Stricker R, Pick R, Storz C, Ritter G and Salmon N 1994 Nonlinear absorption extends confocal fluorescence microscopy into the ultra-violet regime and confines the illumination volume *Opt. Commun.* **104** 223–8
[21] Sheppard C J R and Cogswell C J 1991 Effects of aberrating layers and tube length on confocal imaging properties *Optik* **87** 34–8
[22] Hell S, Reiner G, Cremer C and Stelzer E H K 1993 Aberrations in confocal fluorescence microscopy induced by mismatches in refractive index *J. Microsc.* **169** 391–405
[23] Jacobsen H and Hell S W 1995 Effect of the specimen refractive index on the imaging of a confocal fluorescence microscope employing high aperture oil immersion lenses *Bioimaging* **3** 39–47
[24] Török P, Varga P, Laczik Z and Booker G R 1995 Electromagnetic diffraction of light focused through a planar interface between materials of mismatched refractive indices: an integral representation *J. Opt. Soc. Am.* A **12** 325–32
[25] Wiersma S H and Visser T D 1996 Defocusing of a converging electromagnetic wave by a plane dielectric interface *J. Opt. Soc. Am.* A **13** 320–5
[26] Lanni F 1986 Standing-wave fluorescence microscopy *Applications of Fluorescence in the Biomedical Sciences* ed D L Taylor *et al* (New York: Liss)